

Weighting supermassive black holes

Eugene Vasiliev
LPI astro seminar, 5 June 2013

Overview of mass determination methods

- Active galactic nuclei
 - Spectrum fitting
 - Reverberation mapping
- Quiescent galaxies
 - Observational data
 - Stellar-dynamical methods:
 - Jeans equations
 - Schwarzschild models
 - Individual orbits
 - Gas-dynamical models
 - Maser measurements
- Correlations of black hole mass with other parameters

Spectral fitting to the AGN emission

continuum emission

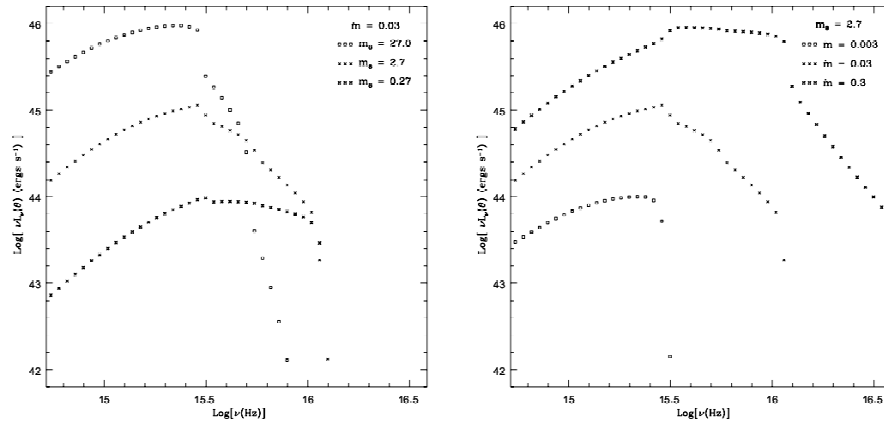
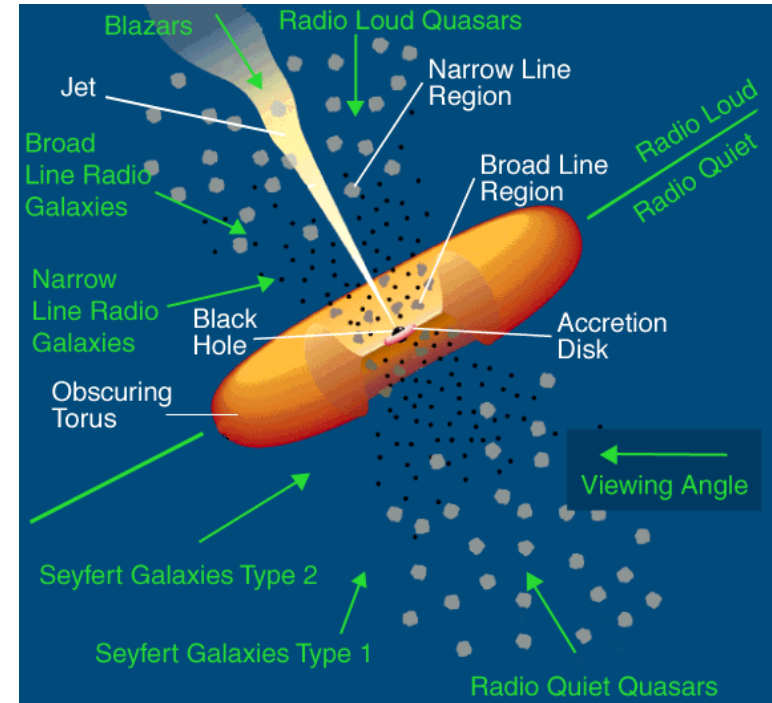
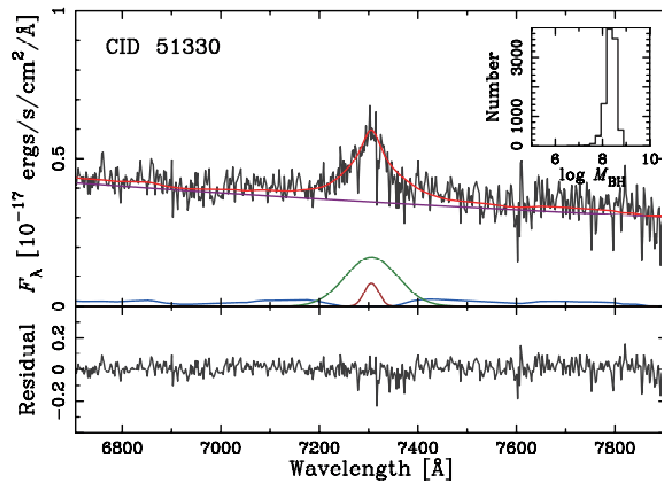


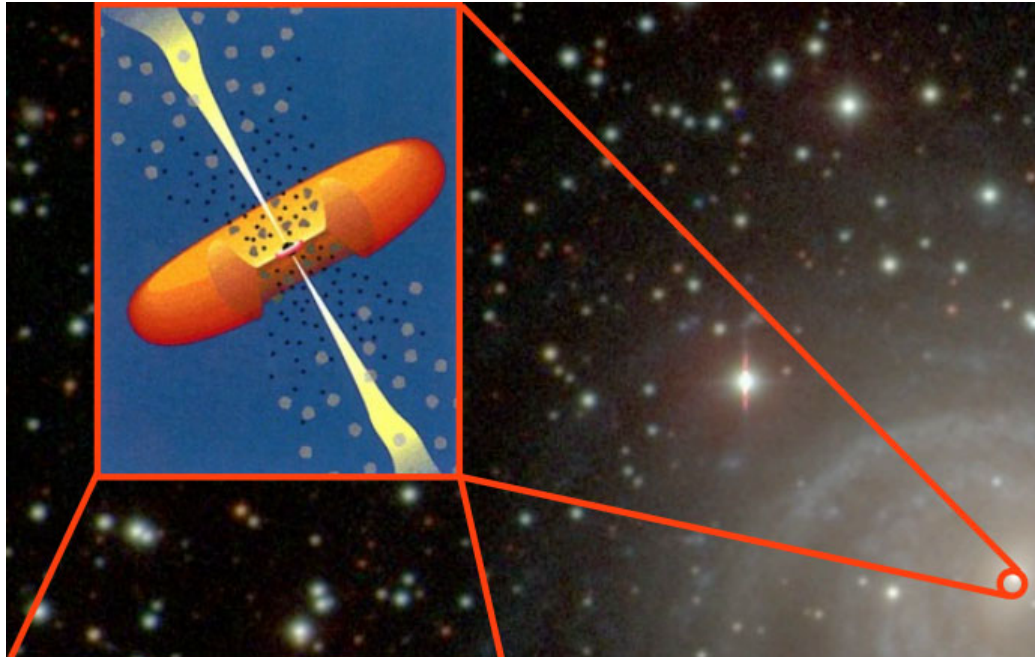
Figure 25. The face-on standard disk spectrum for a fixed mass accretion rate and varying central mass (left) and a fixed central mass and varying accretion rate (right). The models are from Sincell & Krolik (1998).

spectral lines



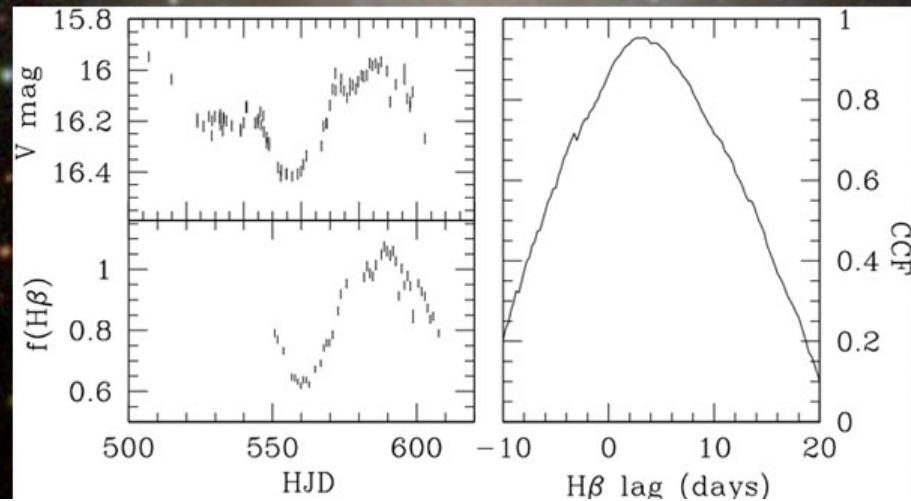
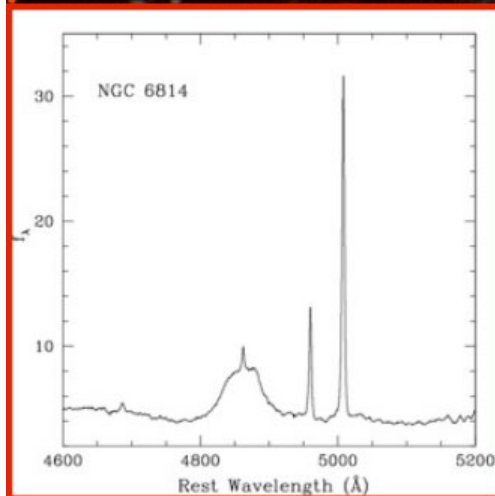
Problems: complex physics of accretion discs, large degeneracy between M_{bh} and accretion rate

Reverberation mapping



Time delay between variability of emission in continuum in the broad-line region (BLR) and line emission in the narrow line region provides information about the size of BLR; the BH mass can be estimated from the

virial relation: $GM = f \sigma^2$, where the geometric factor f depends on the structure of BLR (needs to be calibrated against other techniques of estimating M)



Black holes in quiescent galaxies: observations

Unlike AGN studies, spatially-resolved spectroscopy is crucial for dynamical mass modelling!

The key requirement is the need to resolve the black hole influence radius:

$$r_{\text{infl}}, '' = \frac{G M_{\text{bh}}}{\sigma^2 D} = 2.2'' \left(\frac{M_{\text{bh}}}{10^8 M_{\odot}} \right) \left(\frac{\sigma}{200 \text{ km/s}} \right)^{-2} \left(\frac{D}{1 \text{ Mpc}} \right)^{-1}$$

Observational data

- | | | |
|--|--|---------------------------------------|
| • Stellar dynamics | photometry, spectroscopy –
stellar absorption lines | NIR, optics, ~0.1'' resolution |
| • Gas dynamics | ionized gas emission lines | |
| • Maser sources in gas orbiting the black hole | molecular gas (H ₂ O) emission | 22GHz radio, 10 ⁻³ '' res. |

GALAXIES WITH DYNAMICAL MEASUREMENTS OF M_{\bullet}

Galaxy	M_{\bullet} (+, -) (M_{\odot})	Ref.	σ (km s^{-1})	$\log L_V$	M_{bulge} (M_{\odot})	Ref.	r_{inf} (arcsec)	Morph.	D (Mpc)	Method
Milky Way ^a	4.1 (0.6,0.6) e6	1,2	103 ± 20				43	S	0.008	stars
A1836-BCG	3.9 (0.4,0.6) e9	3	288 ± 14	11.26 ± 0.06			0.27	E (C)	157.5	gas
A3565-BCG	1.4 (0.3,0.2) e9	3	322 ± 16	11.24 ± 0.06			0.22	E (C)	54.4	gas
Circinus	1.7 (0.4,0.3) e6	4	158 ± 18				0.02	S	4.0	masers
IC 1459 ^b	2.8 (1.1,1.2) e9	5	315 ± 16	10.96 ± 0.06	3.07e11	45	0.81	E (C)	30.9	stars
N221 (M32) ^y	2.6 (0.5,0.5) e6	6	75 ± 3	8.52 ± 0.02	7.62e8	45	0.57	E (I)	0.73	stars
N224 (M31) ^y	1.4 (0.8,0.3) e8	7	160 ± 8				6.5	S	0.73	stars
N524 ^w	8.6 (1.0,0.4) e8	8	235 ± 12	10.62 ± 0.04			0.57	S0 (C)	24.2	stars
N821 ^w	1.7 (0.7,0.7) e8	9	209 ± 10	10.36 ± 0.05	1.92e11	9	0.14	E (I)	23.4	stars
N1023 ^w	4.0 (0.4,0.4) e7	10	205 ± 10	10.06 ± 0.11	6.49e10	45	0.08	S0 (pl)	10.5	stars
N1194 ^c	6.8 (0.3,0.3) e7	11	148^{+26}_{-22}				0.05	S0	55.5	masers
N1300	7.1 (3.4,1.8) e7	12	218 ± 10				0.07	S	20.1	gas
N1316 ^x	1.7 (0.3,0.3) e8	13	226 ± 11	11.18 ± 0.05			0.14	E (I)	21.0	stars
N1332 ^w	1.5 (0.2,0.2) e9	14	328 ± 16	10.16 ± 0.05			0.54	S0 (pl)	22.7	stars
N1374 ^{b,x}	5.9 (0.6,0.5) e8	15	174 ± 9	10.10 ± 0.05	5.79e10	15	0.89	E (C)	19.6	stars
N1399 ^{b,d,x}	5.1 (0.6,0.7) e8	16	296 ± 15	10.78 ± 0.04	3.98e11	46	0.25	E (C)	20.9	stars
N1399 ^{b,d,x}	1.3 (0.5,0.7) e9	17	296 ± 15	10.78 ± 0.04	3.98e11	46	0.63	E (C)	20.9	stars
N1407 ^{b,w}	4.7 (0.7,0.5) e9	15	274 ± 14	11.05 ± 0.05	1.00e12	15	1.9	E (C)	29.0	stars
N1550 ^b	3.9 (0.7,0.7) e9	15	289 ± 14	10.87 ± 0.05			0.78	E (I)	53.0	stars
N2273 ^c	7.8 (0.4,0.4) e6	11	144^{+18}_{-15}				0.01	S	26.8	masers
N2549 ^w	1.4 (0.1,0.4) e7	8	145 ± 7	9.55 ± 0.04	1.99e10	8	0.05	S0 (pl)	12.7	stars
N2787 ^w	4.1 (0.4,0.5) e7	18	189 ± 9				0.14	S0 (pl)	7.5	gas
N2960 ^c	1.21 (0.05,0.05) e7	11	166^{+16}_{-15}				0.01	S	75.3	masers
N3031 (M81)	8.0 (2.0,1.1) e7	19	143 ± 7				0.85	S	4.1	gas
N3091	3.7 (0.1,0.5) e9	15	307 ± 15	11.00 ± 0.05			0.66	E (C)	52.7	stars
N3115 ^w	8.9 (5.1,2.7) e8	20	230 ± 11	10.34 ± 0.02	1.57e11	45	1.6	S0 (pl)	9.5	stars
N3227	1.5 (0.5,0.8) e7	21	133 ± 12				0.04	S	17.0	stars
N3245 ^w	2.1 (0.5,0.6) e8	22	205 ± 10		7.00e10	45	0.21	S0 (pl)	21.5	gas
N3368 ^w	7.6 (1.6,1.5) e6	23	122^{+28}_{-24}				0.04	S	10.6	stars
N3377 ^w	1.8 (0.9,0.9) e8	9	145 ± 7	9.93 ± 0.04	2.35e10	9	0.69	E (pl)	11.0	stars

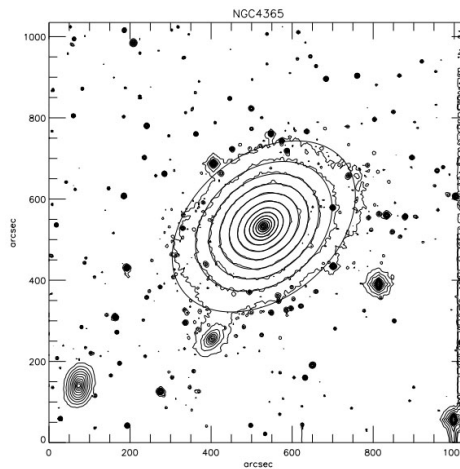
compilation of 72 mass measurements from McConnell & Ma 2013

Stellar-dynamical models: observations

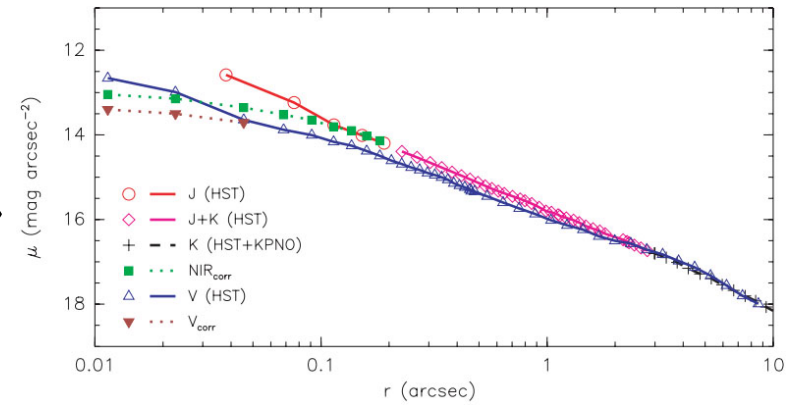
Photometric data



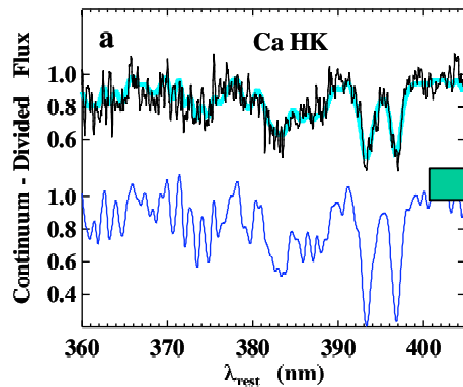
surface brightness map



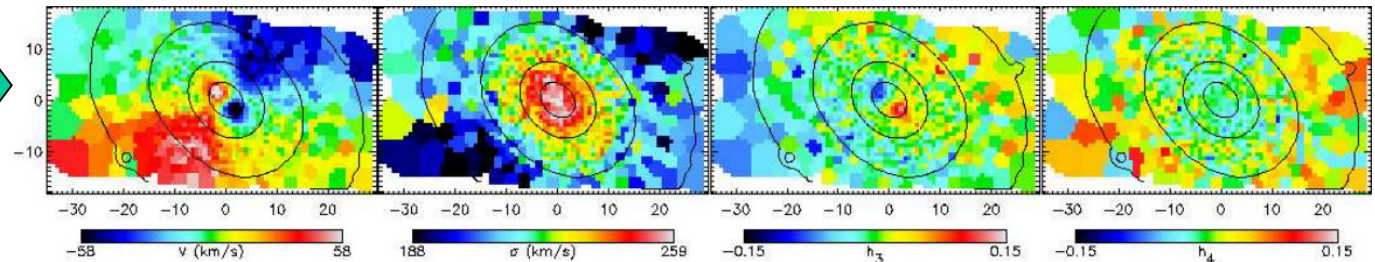
luminosity profile (+flattening)



integral-field spectroscopy

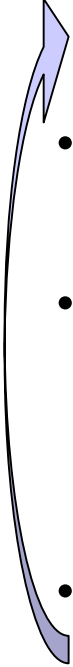


kinematic map (mean velocity, dispersion and higher moments, or full line-of-sight velocity distribution from fitting absorption line profiles)



[a cautionary note: resolved star spectroscopy might give different results, e.g. Lanzoni+ 2013]

Stellar-dynamical models: roadmap

- Obtain surface brightness and kinematic data for the galaxy
 - Deproject surface brightness to obtain 3d mass density $\rho(\vec{r})$
(requires specification of inclination angle(s) and M/L ratio for stars)
 - Take the gravitational potential as the sum of potential created by distribution of stars, central black hole, and possibly dark matter halo
 - Find the distribution function (or its moments) of stars, compute the velocity distribution that it yields
(taking into account telescope PSF and other instrumental effects), compare with observations to obtain the goodness of fit χ^2
 - Repeat with different values of M_{bh} , M/L and other parameters to find the best-fit values and uncertainties for the model parameters
- 

Stellar dynamics: preliminaries

The steady-state distribution function of stars in a galaxy is described by

collisionless Boltzmann equation
$$\frac{\delta f}{\delta t} + \vec{v} \cdot \vec{\nabla} f - \vec{\nabla} \Phi(\vec{x}, t) \cdot \frac{\delta f}{\delta \vec{v}} = 0 \quad (\text{CBE})$$

and Poisson equation

$$\nabla^2 \Phi(\vec{x}, t) = 4\pi G \rho(\vec{x}, t)$$

$f(\vec{x}, \vec{v}, t)$ is a function of 6 variables (+time if it is not stationary).

We can extract at most 3-dimensional data from the observations:
1d line-of-sight velocity distribution at each point in 2d image.

Fortunately, the Jeans theorem tells us that the distribution function may only depend on the integrals of motion, of which there are usually at most 3.

Sadly, not all integrals are known in an explicit form if the potential is not very symmetric.

Moreover, it is not generally possible to derive both the distribution function of stars and the gravitational potential simultaneously in a unique way.

Jeans equations

We can simplify the task by using the moments of CBE over velocity to obtain

the Jeans equation(s); in the spherical case it reads
$$\frac{d(\nu \overline{v_r^2})}{dr} + 2 \frac{\beta}{r} \nu \overline{v_r^2} = -\nu \frac{d\Phi}{dr}$$

where the velocity anisotropy coefficient is
$$\beta \equiv 1 - \frac{\overline{v_\theta^2} + \overline{v_\phi^2}}{2\overline{v_r^2}}.$$

More complex equations can be written for the axisymmetric case [e.g. Cappellari 2008] and integrable triaxial potentials [e.g. van de Ven+ 2003]

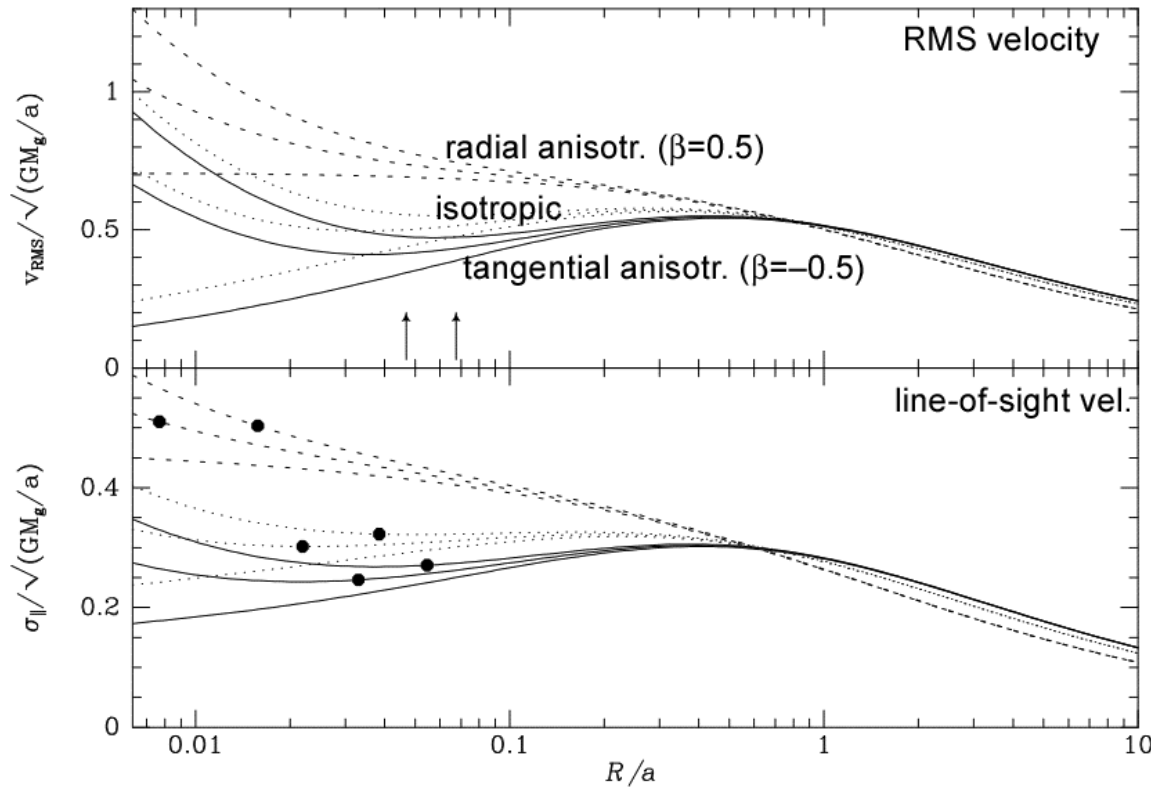
Pros

- easy to deal with
- require only the knowledge of first two moments of vel.distr.

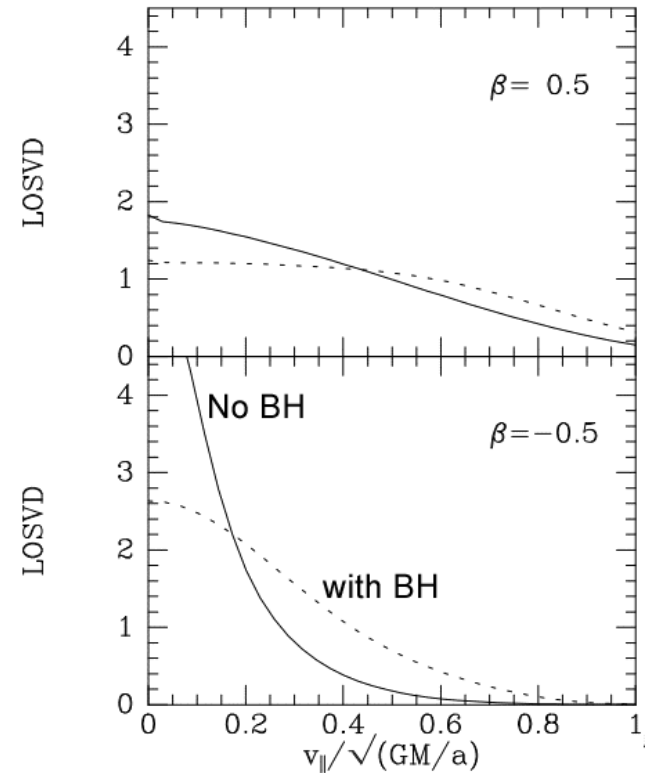
Cons

- equations are not closed (e.g. require the knowledge of β in the spherical case)
- cannot ensure non-negativity of the distribution function
- systematical errors due to imposed form of the solution (e.g. semi-isotropy)

The mass – velocity anisotropy degeneracy



velocity dispersion as a function of radius



line-of-sight vel. distribution

A more radially anisotropic distribution can mimic a larger central point mass, because more stars close to the center will be observed with velocity vectors pointing along the line of sight.

The degeneracy is lifted by using higher-order moments or the full LOSVD (not only the dispersion).

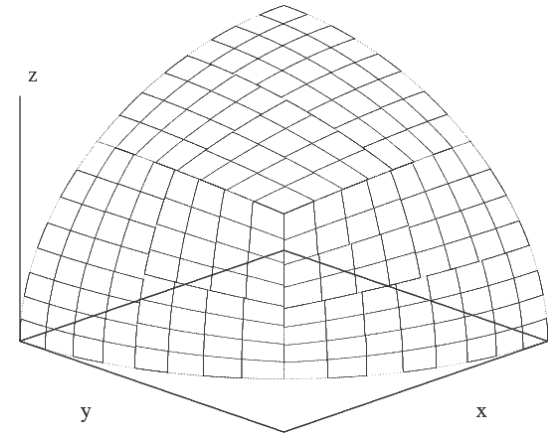
Schwarzschild models

Schwarzschild(1979) introduced a general method to numerically construct self-consistent models with a given density profile in a given (non-spherical) potential

- Take a specified density profile $\rho(\mathbf{r})$ / potential $\Psi(\mathbf{r})$
- Divide space into N_c cells with masses m_c
- Integrate N_o orbits in given potential ($N_o \gg N_c$) and calculate the fraction of time t_{oc} that o -th orbit spends in c -th cell
- Solve optimization problem:
find orbit weights $w_o \geq 0$ so that

$$\sum_{i=1}^{N_o} w_o t_{oc} = m_c \quad c = 1..N_c \quad (\text{self-consistency constraints are satisfied})$$

and the kinematical constraints from observations are fulfilled



Schwarzschild models

Pros

- do not require assumptions about velocity anisotropy
- ensure positive distribution fnc.
- applicable in any geometry (most studies so far considered axisymmetric cases), no a priori knowledge about integrals of motion is required
- potentially less prone to systematic errors due to artificially imposed restrictions on the form of distribution fnc

Cons

- computationally expensive
- restriction on the modelling technique (e.g. assumption of axisymmetry or constant M/L) may induce unknown systematics and artificially reduce uncertainties

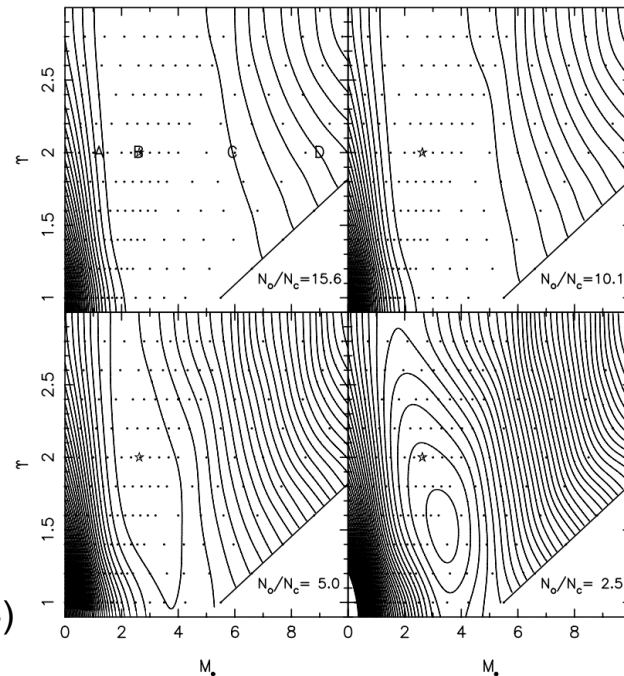
Recent improvements

- inclusion of dark matter halo
- radial variation of M/L
- triaxiality

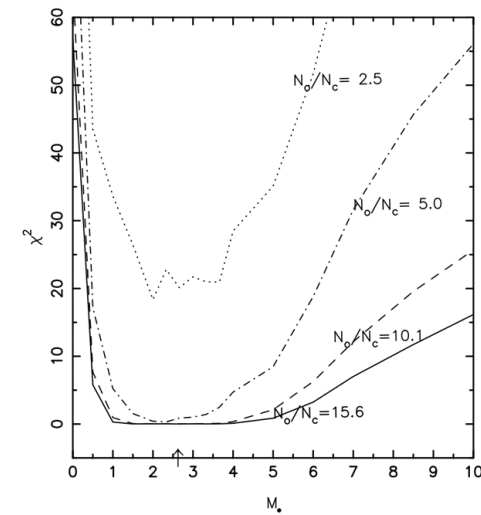
Degeneracy of mass determination

- A sufficiently flexible method for constructing the distribution function that satisfies a given set of observational constraints will reproduce these constraints with different forms of assumed gravitational potential
- Therefore, the problem of determining M_{bh} is intrinsically ill-conditioned
- A method which is not flexible enough will select a formally unique best-fit solution out of a wider range of equally good possibilities, thereby artificially reducing uncertainties of mass determination

2d contour plots of χ^2 as a function of M_{bh} and M/L , for different sizes of orbit library



(Valluri, Merritt & Emsellem 2004)



Flat-bottomed χ^2 plots are almost never seen in published papers!

The special case of Milky Way: monitoring orbits of individual stars

probed distances are ~ 5000 times smaller than influence radius!

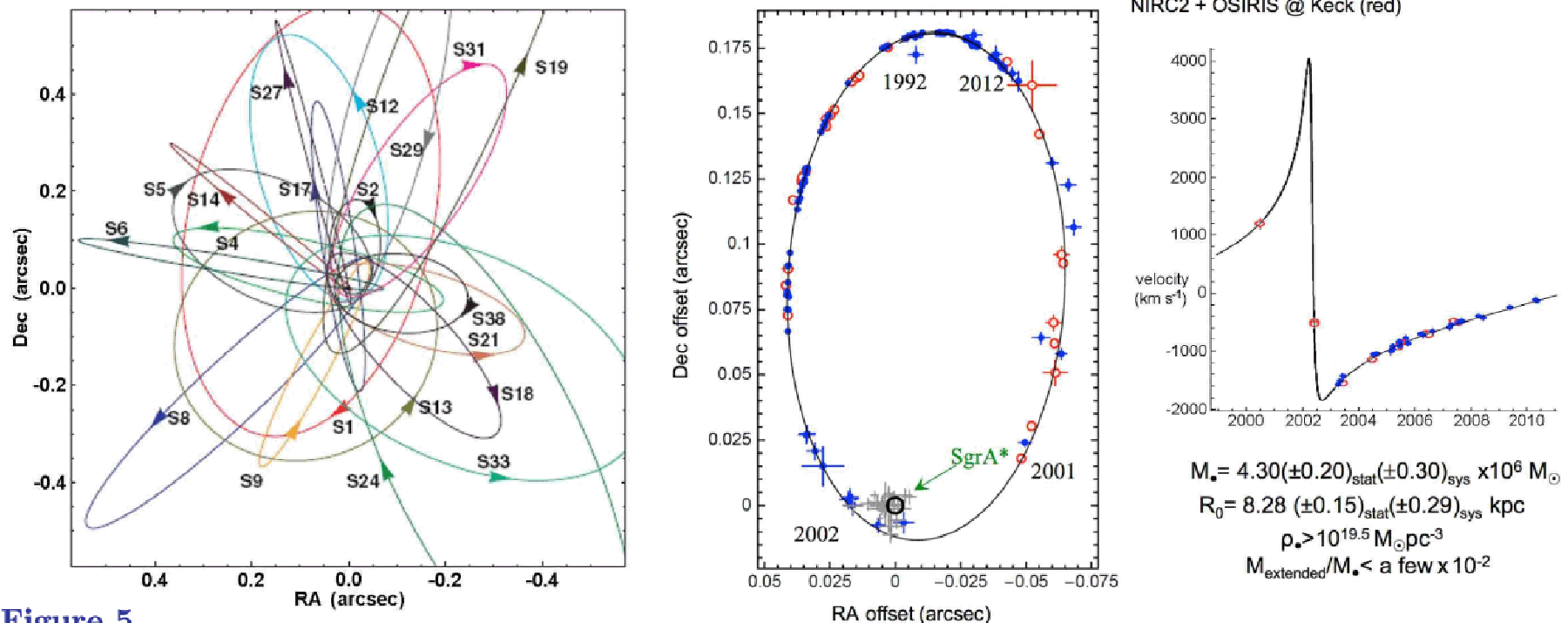
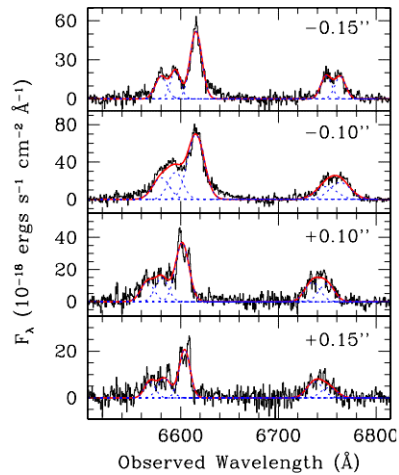


Figure 5

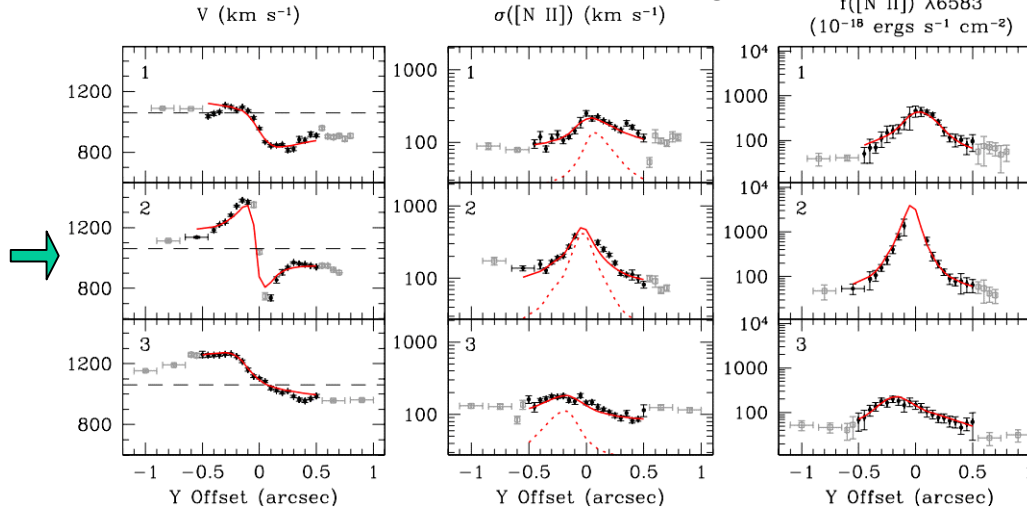
(left) Orbits of individual stars near the Galactic center. (right) Orbit of star S2 around the BH and associated radio source Sgr A* based on observations of its position from 1992 to 2012. Results from the Ghez group using the Keck telescope and from the Genzel group using the European Very Large Telescope (VLT) are combined.

Gas kinematical models

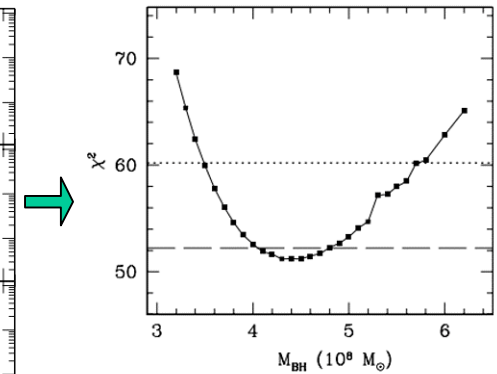
fit emission spectra



determine the kinematics of gas disc



find best-fit M_{bh}



(Walsh et al.2010 for M84)

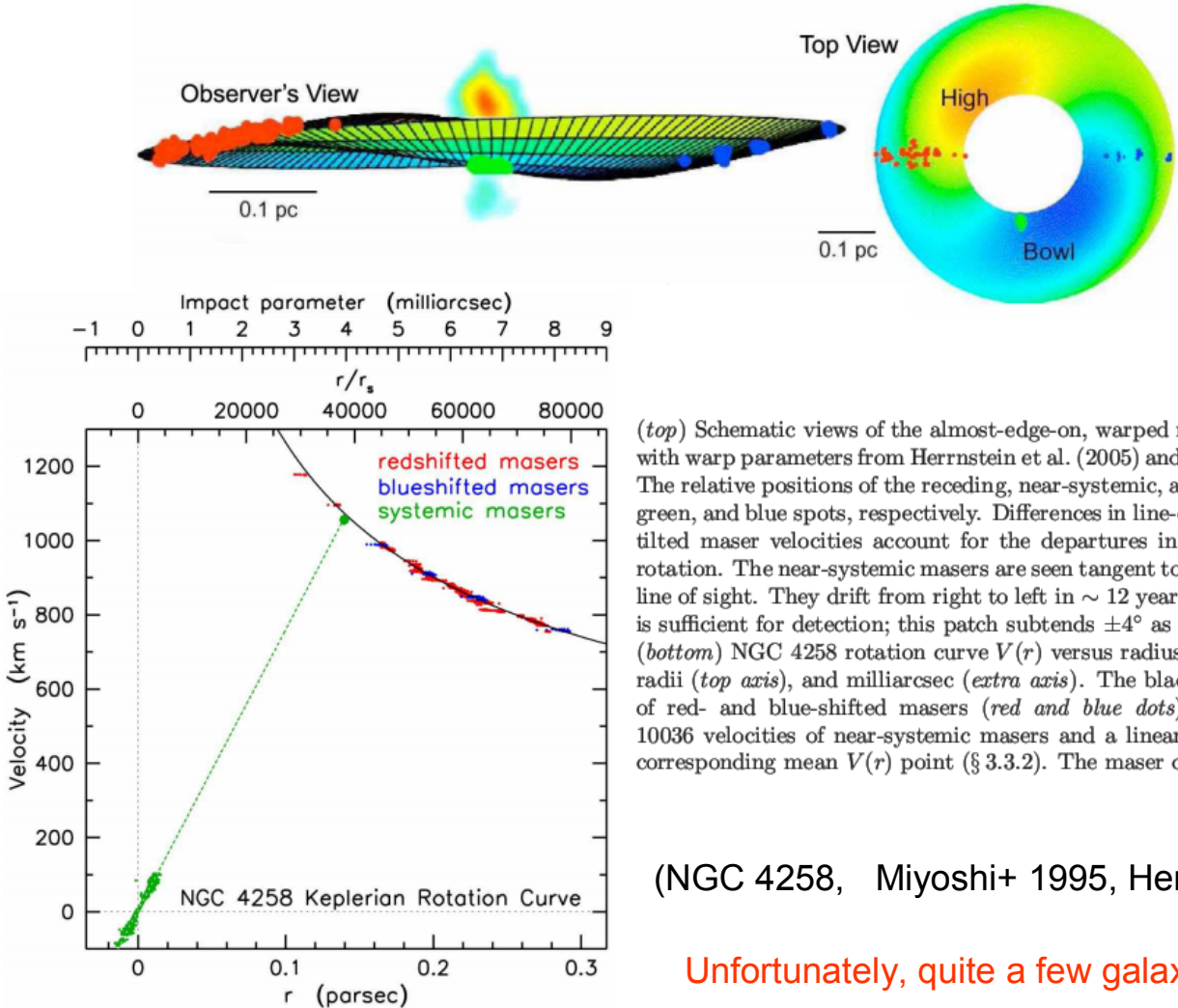
Pros

- no problem with velocity anisotropy – gas is on a circular Keplerian orbit
- violation of model assumptions (e.g. disc is not cold or warped) is easily verified

Cons

- dust often accompanies gas
- gas is often influenced by non-gravitational forces (pressure, turbulence, magnetic fields)
- many galaxies do not demonstrate a sufficiently ordered motion for the gas-dynamical modelling to be successful

Maser sources in molecular gas



(top) Schematic views of the almost-edge-on, warped maser disk of NGC 4258 (from Moran 2008) with warp parameters from Herrnstein et al. (2005) and including the inner contours of the radio jet. The relative positions of the receding, near-systemic, and approaching masers are indicated by red, green, and blue spots, respectively. Differences in line-of-sight projection corrections to the slightly tilted maser velocities account for the departures in the high- $|V|$ masers from exact Keplerian rotation. The near-systemic masers are seen tangent to the bottom of the maser disk bowl along the line of sight. They drift from right to left in ~ 12 years across the green patch where amplification is sufficient for detection; this patch subtends $\pm 4^\circ$ as seen from the center (Moran 2008).

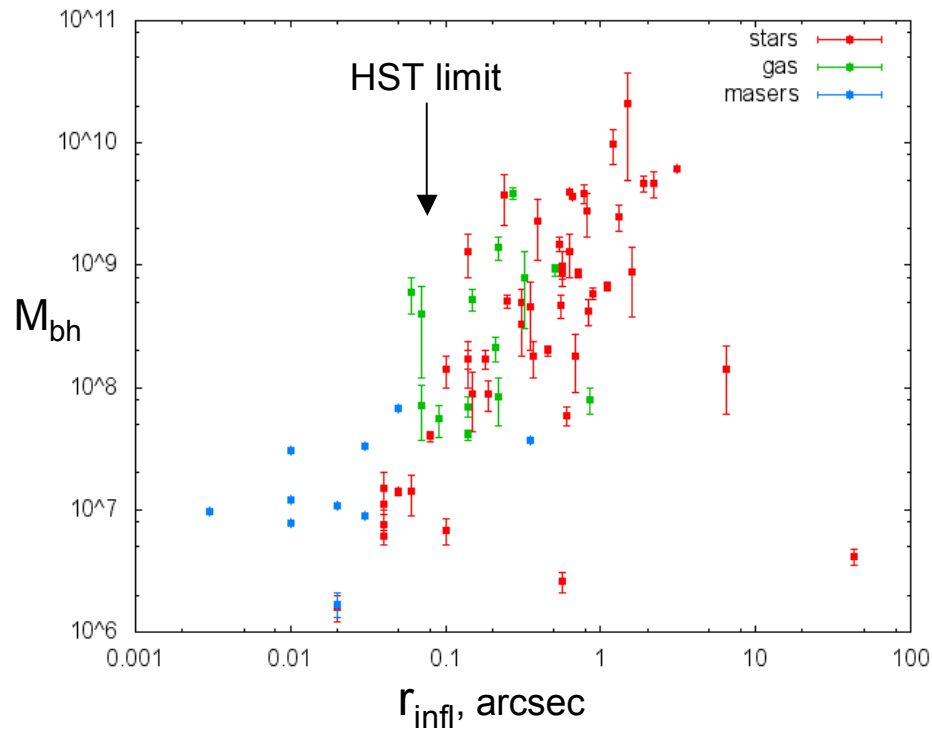
(bottom) NGC 4258 rotation curve $V(r)$ versus radius in units of pc (bottom axis), Schwarzschild radii (top axis), and milliarcsec (extra axis). The black curve is a Keplerian fit to 4255 velocities of red- and blue-shifted masers (red and blue dots). The small green points and line show 10036 velocities of near-systemic masers and a linear fit to them. The green filled circle is the corresponding mean $V(r)$ point (§ 3.3.2). The maser data are taken from Argon et al. (2007).

(NGC 4258, Miyoshi+ 1995, Herrnstein+ 1999)

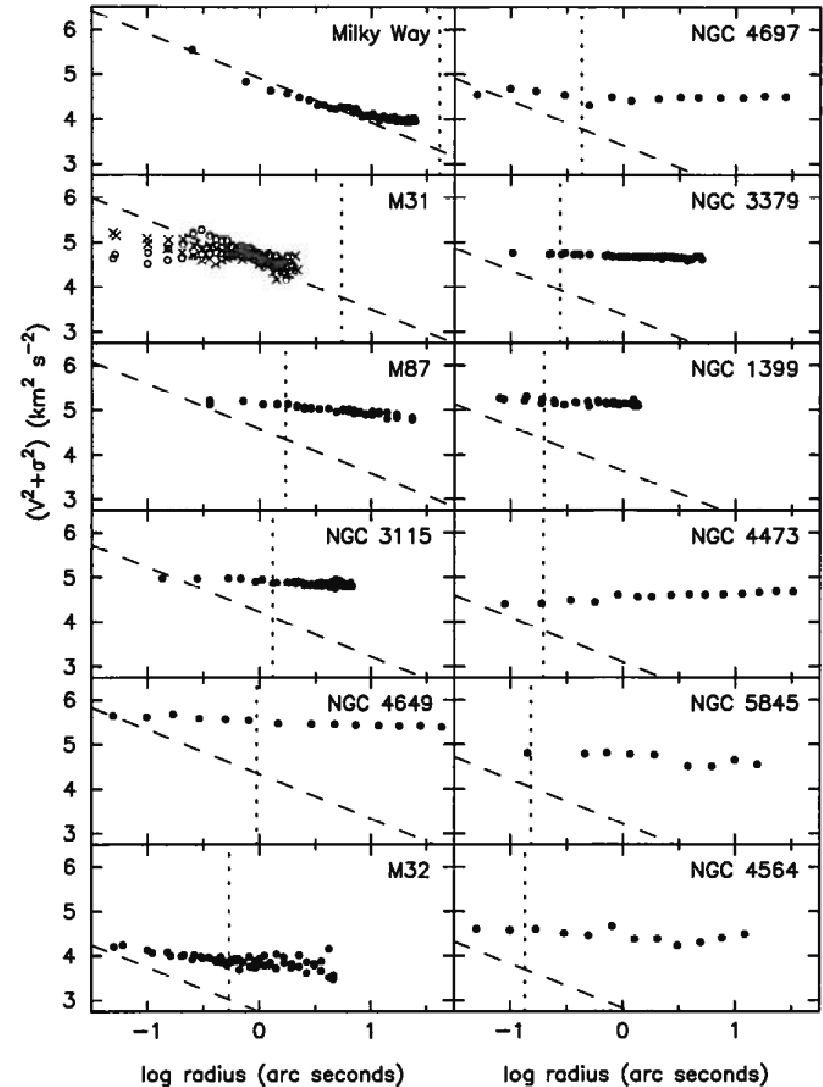
Unfortunately, quite a few galaxies have nuclear maser sources

(figure taken from Kormendy&Ho 2013)

Resolution vs. influence radius

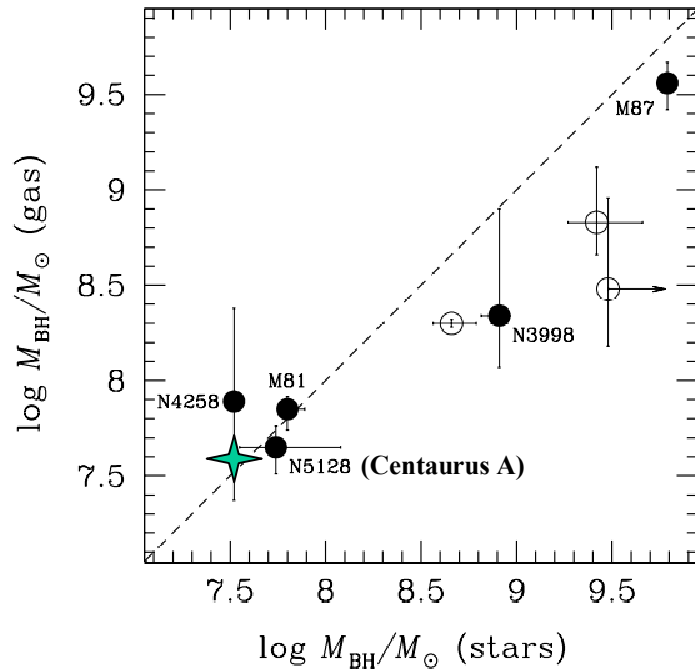


(data from McConnell&Ma 2013)



rise in vel. disp. is rarely seen (Merritt 2013)

Comparison of measurements made with different methods



stellar vs. gas kinematics

AGN

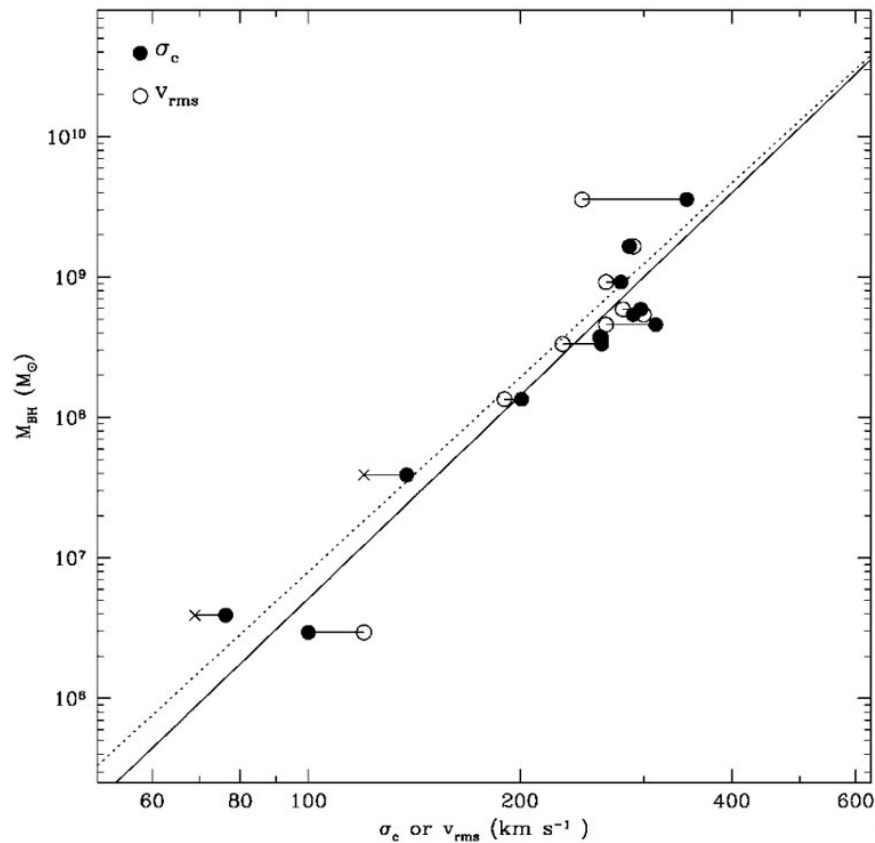
normal galaxies

Method & Telescope	Scale (R_S)	No. of SBH Detections	M_{\bullet} Range (M_{\odot})
Fe K α line (XEUS, ConX)	3-10	0	N/A
Reverberation Mapping (Ground based optical)	600	36	$10^6 - 4 \times 10^8$
Stellar Proper Motion (Keck, NTT, VLT)	1000	1	4×10^6
H ₂ O Megamasers (VLBI)	10^4	1	4×10^7
Gas Dynamics (optical) (Mostly <i>HST</i>)	10^6	11	$7 \times 10^7 - 4 \times 10^9$
Stellar Dynamics (Mostly <i>HST</i>)	10^6	17	$10^7 - 3 \times 10^9$

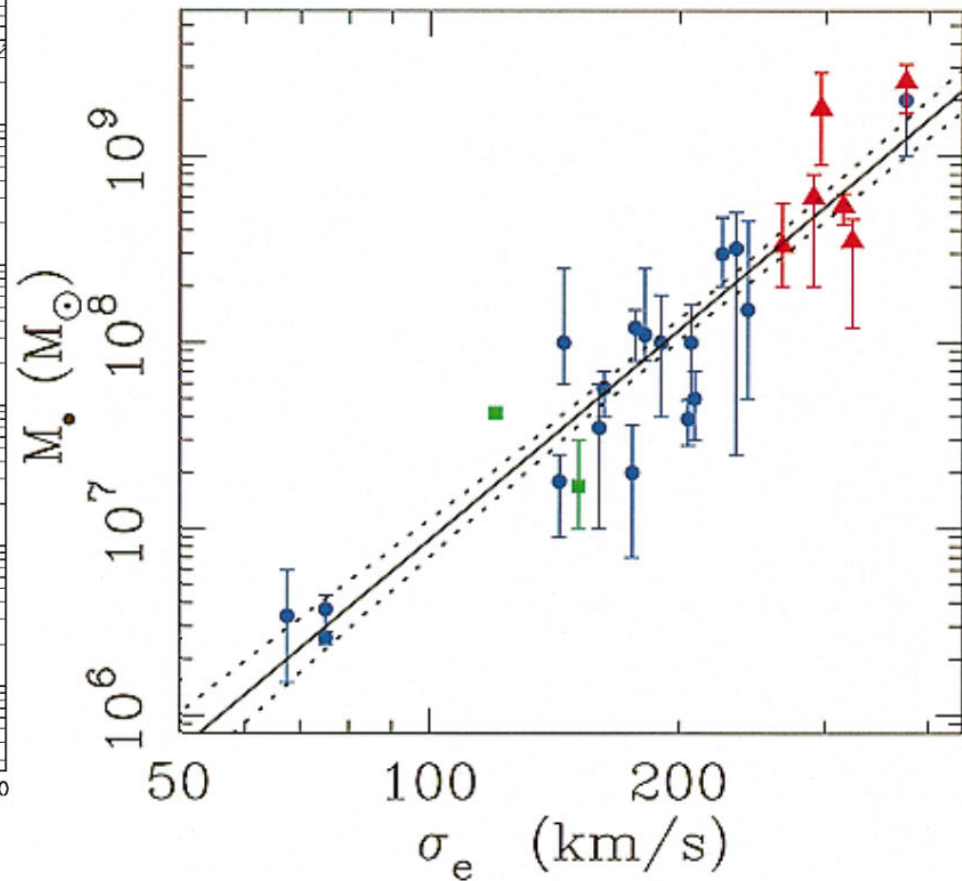
(Ferrarese&Ford 2005, numbers are obsolete)

$M_{\text{bh}}-\sigma$ correlation

$$\lg M_{\text{bh}} = \alpha + \beta \lg(\sigma/200 \text{ km/s}), \quad \alpha \approx 8, \quad \beta \approx 4 \div 5$$

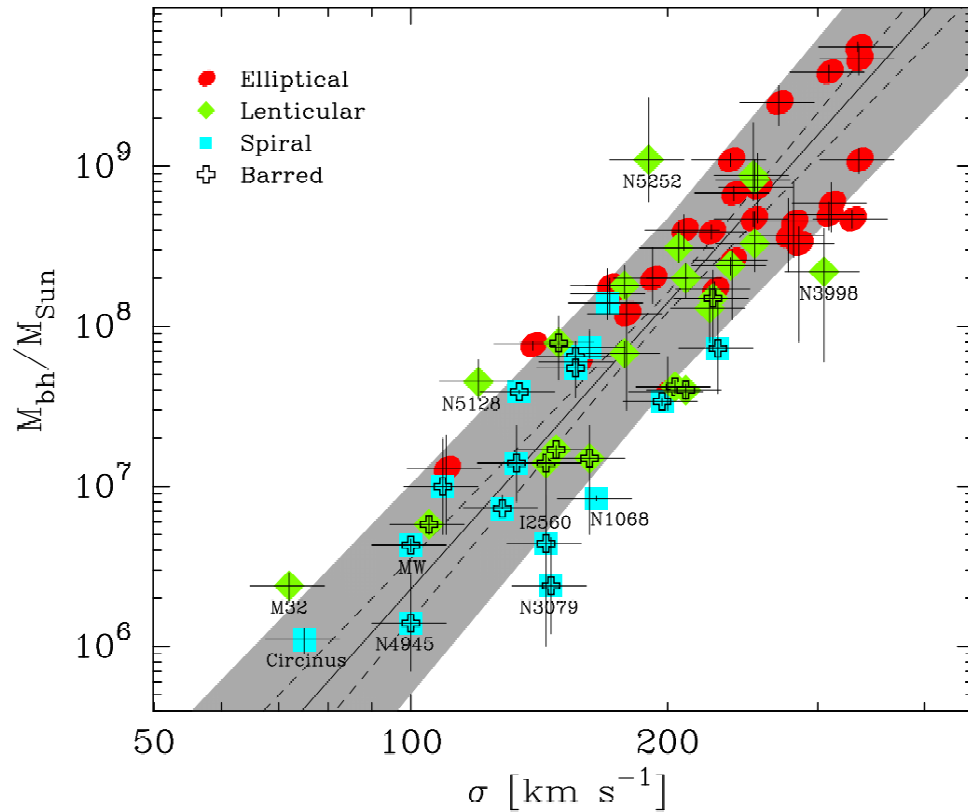


[Ferrarese&Merritt 2000]

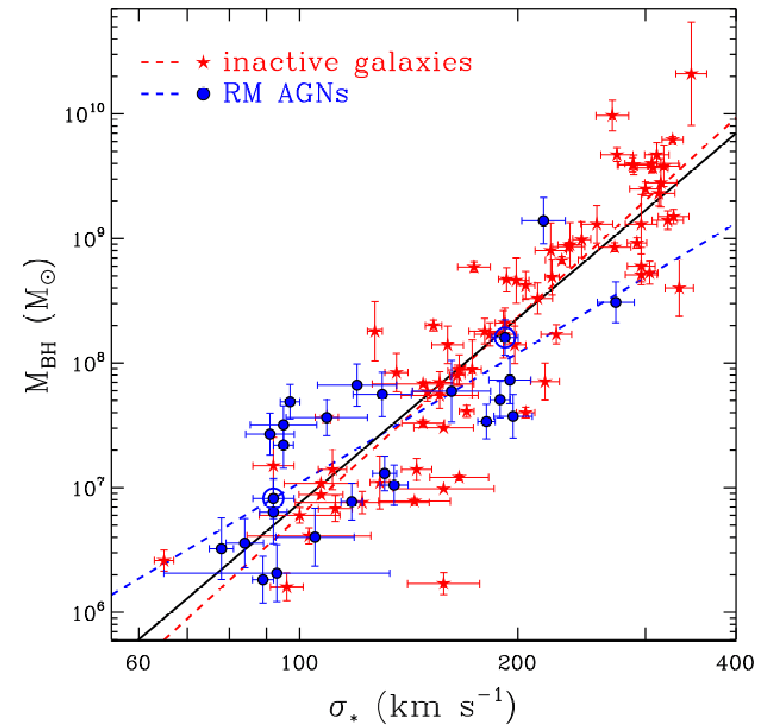


[Gebhardt et al.2000]

$M_{\text{bh}}-\sigma$ correlation



current version: 72 measurements of M_{bh}
(McConnell&Ma 2013)



comparison of masses derived from
reverberation mapping and from stellar
dynamics can be done only on average

$M_{\text{bh}}-\sigma$ correlation

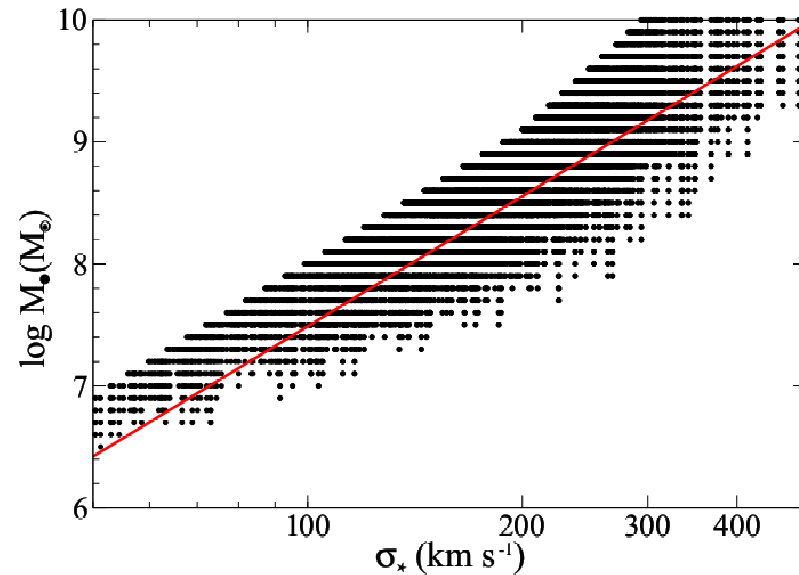
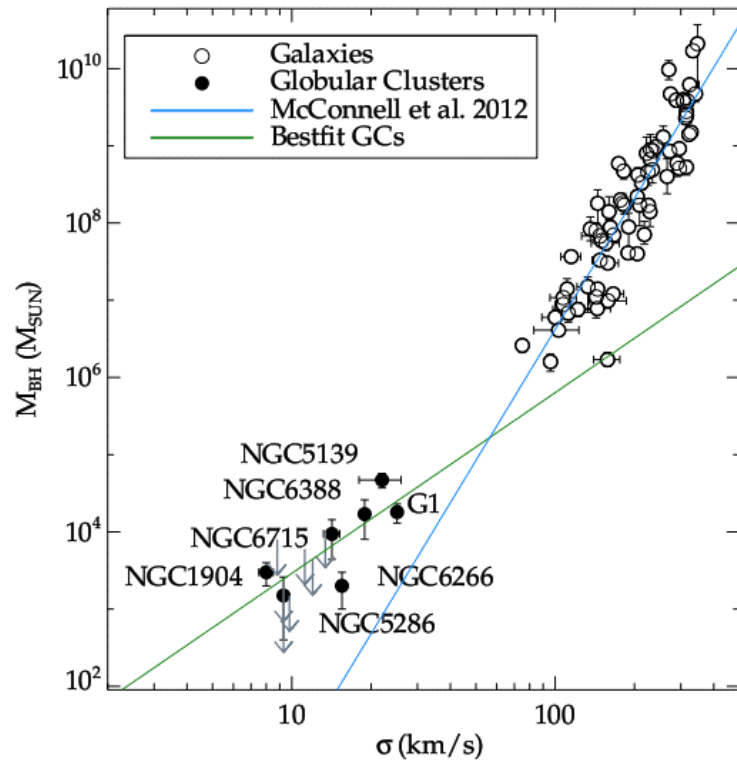


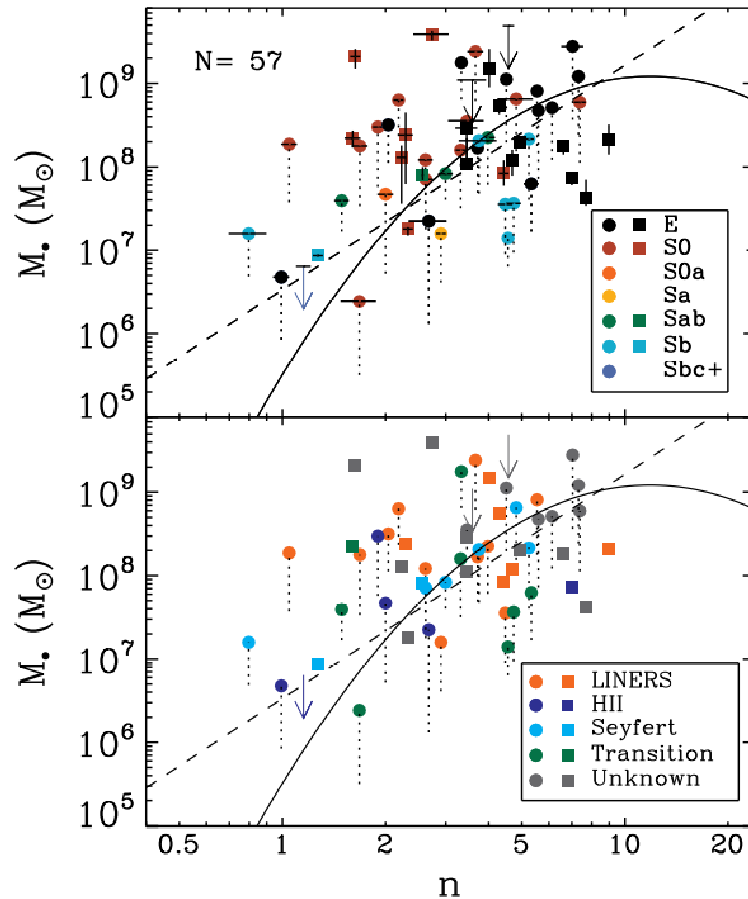
FIG. 2.— Simulated $M_{\bullet} - \sigma_{*}$ data points (black circles) based on a $\mathcal{R} = 0.1$ criteria. This demonstrates the *observable* region of the $M_{\bullet} - \sigma_{*}$ plane with the assumption that there is no $M_{\bullet} - \sigma_{*}$ relation. The fitted $M_{\bullet} - \sigma_{*}$ relation (red line) is $\alpha = 8.4, \beta = 3.5$.

possible downward extension to IMBHs
globular clusters? (Lutzgendorf+ 2013)

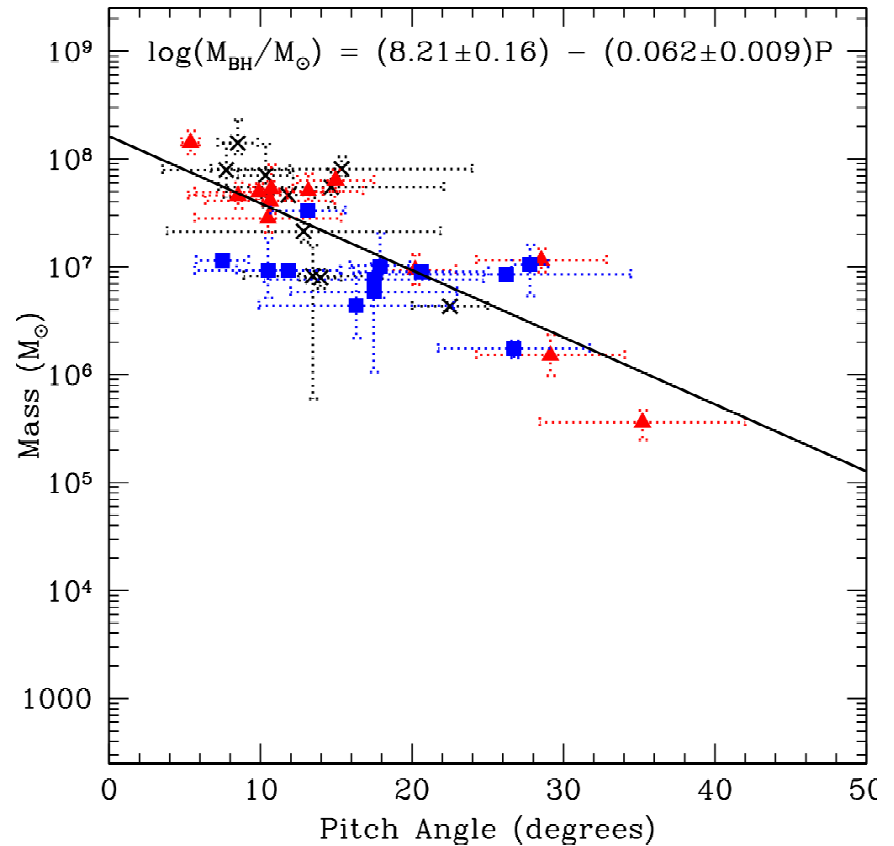
relation to other objects (nuclear star
clusters, circumnuclear discs, etc..) ?

could it be an upper limit induced by
observational selection effects?
(Batcheldor 2010)

Other exotic correlations

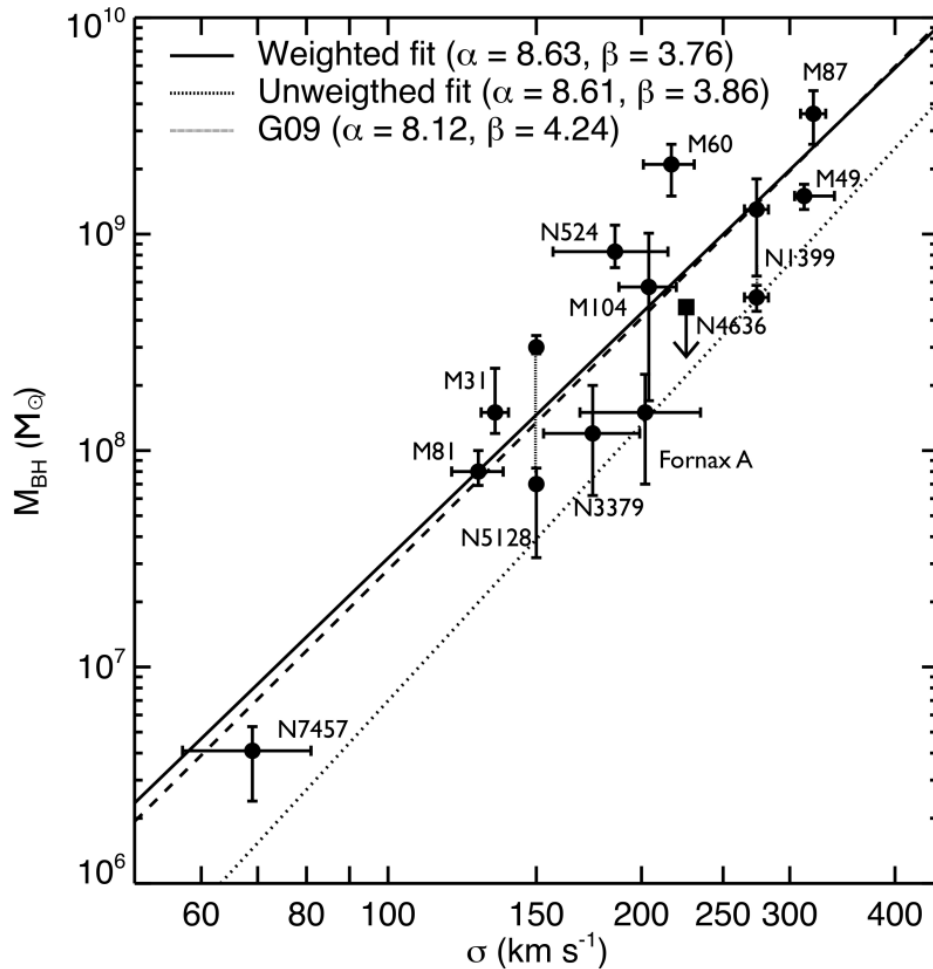


M_{bh} – Sérsic index of bulge [\sim concentration]
(Graham&Driver 2007; disputed...)

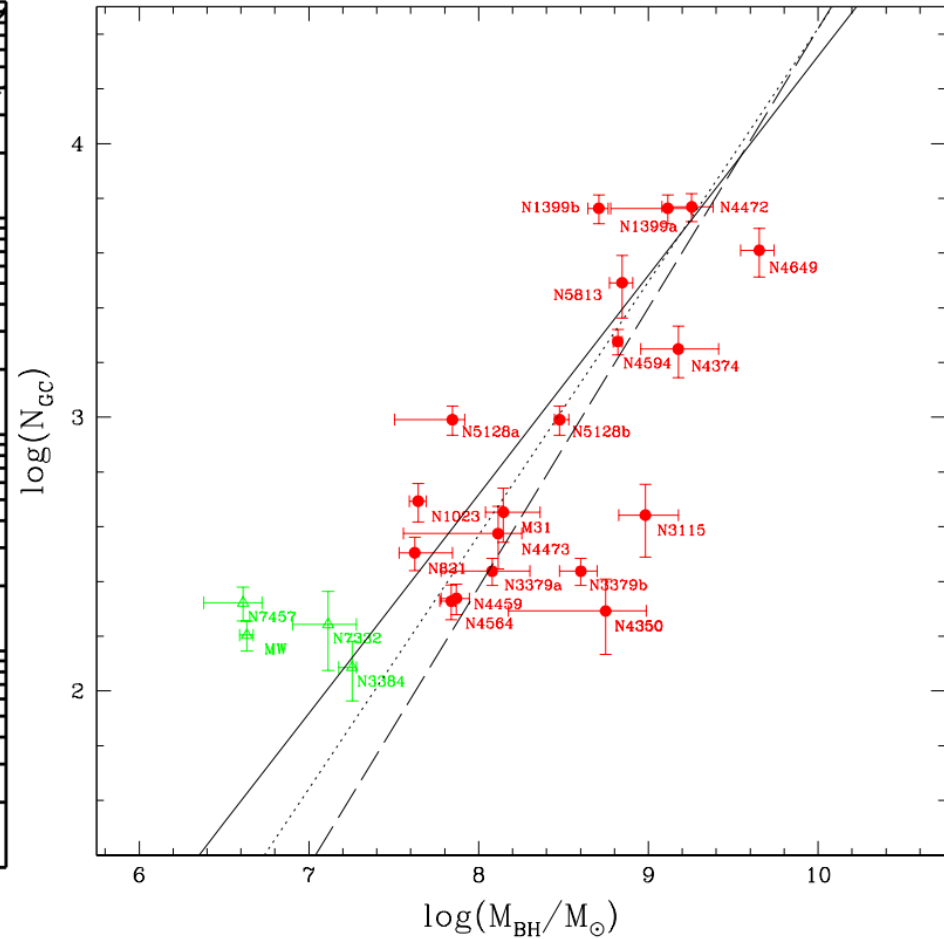


M_{bh} – pitch angle of a spiral galaxy
(Seigar+ 2008, Berrier+ 2013)

Other exotic correlations

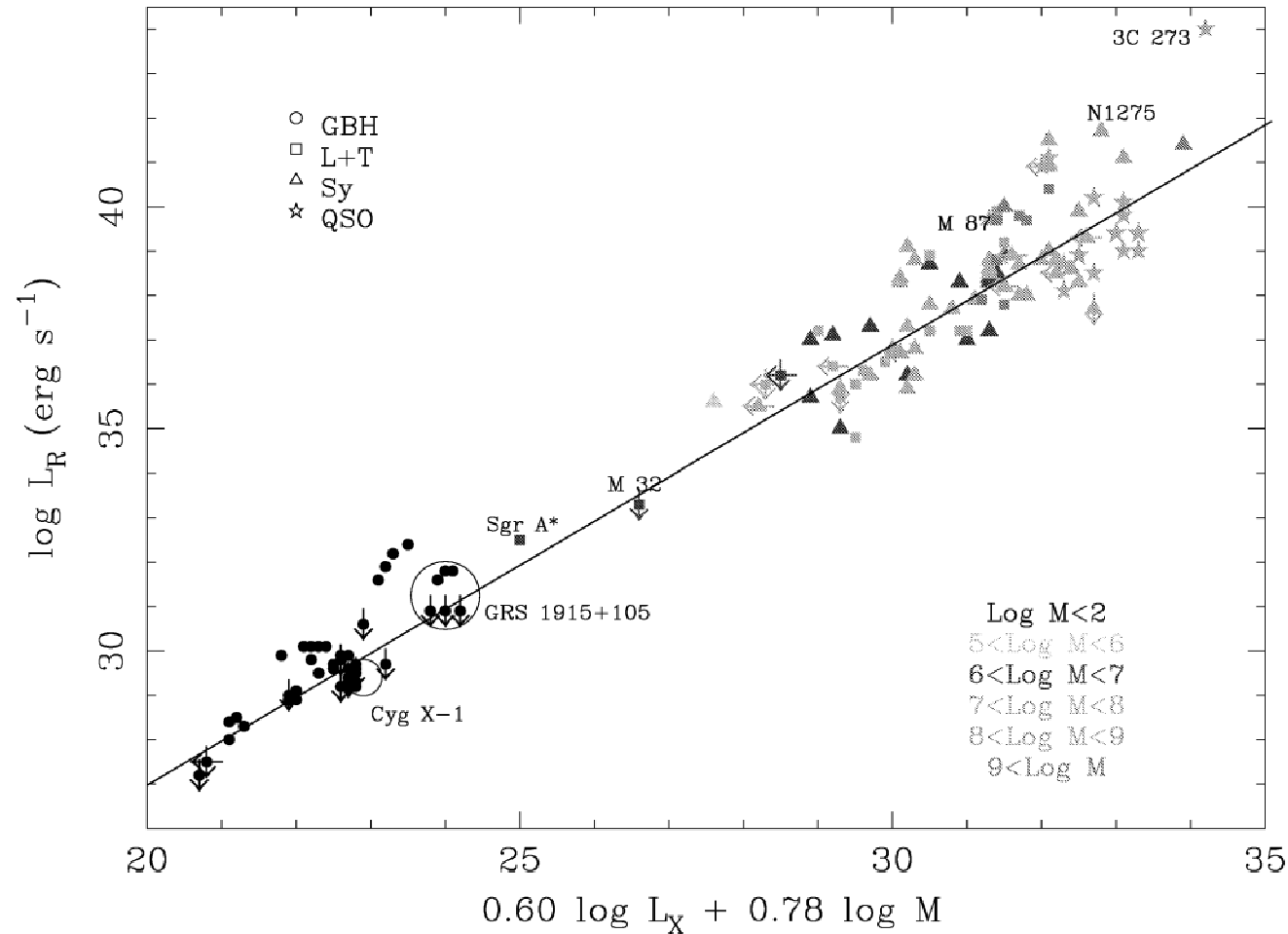


M_{bh} – velocity dispersion of globular cluster systems (Sadoun&Colin 2012)



M_{bh} – number of globular clusters (Rhode 2012, Harris&Harris 2011)

Fundamental plane of active black holes



$$\log L_R = (0.60^{+0.11}_{-0.11}) \log L_X + (0.78^{+0.11}_{-0.09}) \log M + 7.33^{+4.05}_{-4.07} \quad (\text{Merloni+ 2003})$$

radio luminosity X-ray lum. BH mass

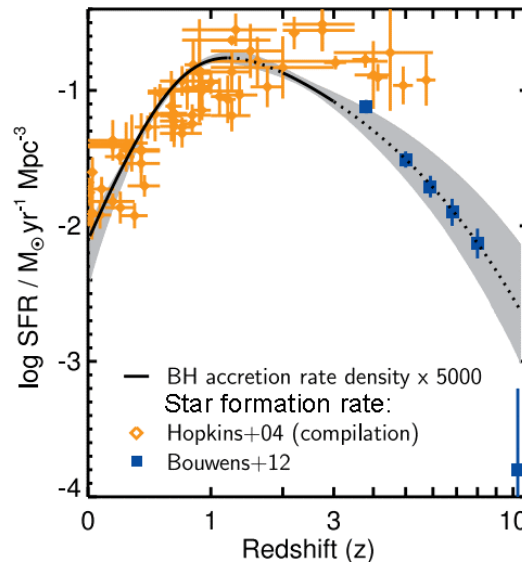
Theoretical explanations for correlations

- Corollary of other scaling relations: Faber-Jackson law – $L \sim \sigma^4$, $M_{\text{bulge}} \sim L^{5/4}$, $M_{\text{bh}} \sim M_{\text{bulge}} \dots$?
- Tidal disruption and accretion of stars in a steep triaxial cusp: $M_{\text{bh}} \sim \sigma^5$ [Merritt&Poon 2004]
- Feedback from initial BH formation and gas accretion [Silk&Rees 1998]:

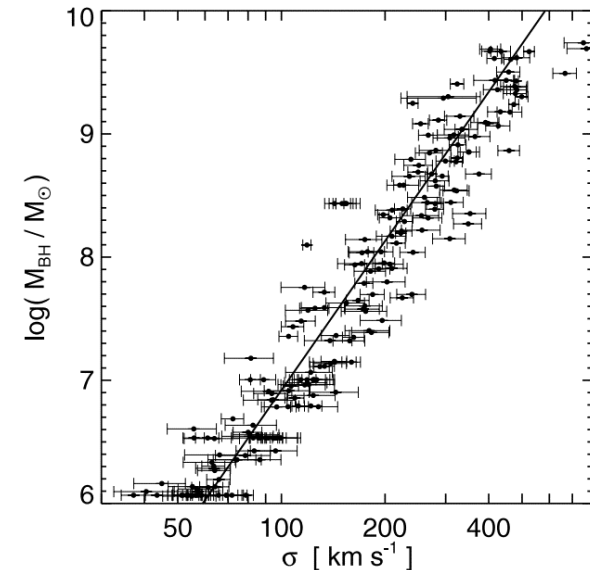
$$L_E = \frac{4\pi GM_\bullet m_p c}{\sigma_e}, \quad (fL_E) \times T_D \approx \frac{GM_{\text{bulge}}^2}{R_{\text{bulge}}}, \quad GM_{\text{bulge}} \approx \sigma^2 R_{\text{bulge}}, \quad T_D \approx R_{\text{bulge}}/\sigma, \quad M_\bullet \approx f^{-1} \frac{\sigma_e \sigma^5}{4\pi G^2 c m_p} \propto \sigma^5.$$

- A more complex coevolution of black holes and their host galaxies, in particular, AGN feedback on the star formation rate; probably involving different modes of feedback (quasar mode, radio mode, ...) [see Kormendy&Ho 2013 for a recent review]

- Need to maintain tightness of the relation in mergers!



Star formation rate vs. BH accretion rate (Aird+ 2010)



Simulated $M_{\text{bh}}-\sigma$ relation (Hopkins+ 2007)

Summary

- Black holes in AGN certainly exist, but their masses are usually estimated to within a factor of few; only the statistical properties are well-defined.
- Black holes in quiescent galaxies are found with a variety of methods (stellar dynamics, gas kinematics, maser sources). These methods depend on the ability to spatially resolve the BH influence radius.
- Most of the methods have quite large, perhaps underestimated, systematic uncertainties. Agreement between measurements made with different methods, or between successive models of the same object, is to within a factor of few.
- Black hole masses correlate with various properties of host galaxies, most notably, velocity dispersion of the spheroidal component.
- Theoretical understanding of these relations is still lacking; they probably involve various feedback mechanisms at different stages of (co)evolution.